EPJ Web of Conferences **71**, 00052 (2014)
DOI: 10.1051/epjconf/20147100052

Highlights from T2K

David Hadley[1,a] on behalf of the T2K collaboration

[1] *University of Warwick, CV4 7AL, United Kingdom*

Abstract.
T2K is a long baseline neutrino oscillation experiment. A high intensity proton beam at J-PARC produces a narrow-band muon-neutrino beam with a peak energy of 0.6 GeV at the far detector, Super-Kamiokande, 295km from the production point. The T2K experiment has observed electron neutrino appearance in a muon neutrino beam and measured $\sin^2 2\theta_{13} = 0.140^{+0.038}_{-0.032}$ ($0.170^{+0.045}_{-0.037}$) assuming the normal (inverted) hierarchy. In addition the latest measurements of θ_{23} and Δm^2_{32} are reported, along with the latest T2K neutrino interaction cross section measurements of the inclusive CC, CCQE and NCE channels.

1 Introduction

In the standard 3 neutrino model, the flavour states are related to the mass states through the PMNS matrix [1][2]. This mixing matrix is conventionally parameterised by three real mixing angles (θ_{12}, θ_{23}, θ_{13}) and one complex CP violating phase (δ_{CP}). The oscillation probability also depends on the neutrino mass splittings, $\Delta m^2_{ij} = m^2_i - m^2_j$. In the T2K experiment [3] a mostly ν_μ beam with a peak energy of 0.6 GeV is directed towards the Super-Kamiokande detector at a distance of 295 km from the source. The appearance channel ($\nu_\mu \rightarrow \nu_e$) is sensitive to θ_{13}. The disappearance channel ($\nu_\mu \rightarrow \nu_\mu$) is sensitive to θ_{23} and Δm^2_{23}. This note reports the observation of the $\nu_\mu \rightarrow \nu_e$ channel and the consequent measurement of θ_{13}. The measurement of non-zero θ_{13} opens the way to measurement of δ_{CP}. In addition, the latest results from the $\nu_\mu \rightarrow \nu_\mu$ channel and neutrino interaction cross section measurements are reported.

2 The T2K Experiment

A high intensity 30 GeV proton beam at J-PARC is directed towards a graphite target. The charged hadrons produced are focussed by magnetic horns to produce a mostly ν_μ beam. The far detector is located 2.5° degrees off-axis. This exposes the far detector to a narrow-band beam peaked at 0.6 GeV which is optimised to give the maximum appearance probability and the minimum background to the ν_e appearance analysis. The predicted flux at the ND280 near detector is shown in fig. 1. The beam prediction is based on simulations tuned to external

[a] e-mail: d.r.hadley@warwick.ac.uk

hadron production data from the NA61/SHINE experiment [4][5] and in-situ measurements from muon monitors. A total of 6.6×10^{20} POT was delivered up to 2013.

The near detector complex at 280m from the target consists of two main detectors, INGRID (on-axis) and ND280 (off-axis), providing a range of target materials and detector technologies. Their purpose is two-fold. First to directly measure the neutrino beam. Second to measure neutrino interaction cross sections.

INGRID [6] consists of an array of 16 iron/scintillator sandwich modules and a single fine grained pure scintillator detector. The modules cover a range of $x - y$ positions allowing measurement of the profile of the neutrino beam. As well as monitoring the neutrino beam INGRID will also be used to measure neutrino cross sections.

The off-axis near detector, shown in fig. 2, is divided into a Tracker and π^0 detector region. The Fine Grained Detector [7] (FGD1) consists of layers of plastic scintillator bars, 10×10 mm in cross section, read out with wavelength shifting fibers into Multi-Pixel Photon Counters (MPPCs). It provides target mass and track reconstruction near the interaction vertex. The Time Projection Chambers [8] (TPCs) provide PID based on $\mathrm{d}E/\mathrm{d}x$ in the Argon based gas and momentum measurement from track curvature in the magnetic field.

The π^0 detector [9] (P0D) consists of alternating layers of plastic scintillator bars[1], water bags and brass/lead sheets surrounded by e. m. calorimeters. Its main goal is to measure interactions producing π^0 in the final state.

Charged current ν_μ interactions are selected by requiring a reconstructed muon originating in the FGD fiducial volume. Final state charged pions are identified by late charge deposits from decay electrons or additional reconstructed tracks with $\mathrm{d}E/\mathrm{d}x$ consistent with a pion. The event sample is divided into three topologies based on the number of pions reconstructed in the final state: CC0π, CC1π and other. The reconstructed muon momentum is shown in fig. 3. The prior beam flux and neutrino interaction model is fitted to the observed muon $p - \cos(\theta)$ distribution of these samples. This choice of topologies allows the data to constrain the parameters of the interaction model governing quasi-elastic scattering and resonant pion production. The post-fit model with reduced total uncertainty is propogated to the far detector oscillation analyses.

The far detector, Super-Kamiokande (SK), shown in fig. 4, is a 50kt Water Cherenkov detector located 1km underground in the Mozumi Mine in Kamioka. The detector contains $\sim 13,000$ PMTs that image the neutrino interactions. Analysis of the reconstructed Cherenkov rings allows determination of charged lepton flavour and hence the initial neutrino flavour.

3 Oscillation Analysis

3.1 ν_e Appearance

Fully contained, electron-like single ring events are selected. Events with late time signals or electron momentum less than 100 MeV are rejected to remove decay electrons from μ and π. Events with reconstructed neutrino energy $E_{\mathrm{reco}} > 1250$ MeV are rejected as these are mostly intrinsic beam background.

A new PID algorithm improves the π^0 rejection compared to previous T2K analyses. For each PMT, the expected hit charge and time PDF for a given particle species, position and momentum is computed. A combined likelihood is formed from the product over all PMTs and all particles in the case of multiple particle final states such as $\pi \to \gamma\gamma$. A maximum likelihood

[1] readout with the same MPPCs.

fit is performed for each particle hypothesis. The reconstructed position and momentum is taken from the best-fit parameters. The minimized likelihood value is used to determine the particle species. π^0 background is rejected by cutting on the reconstruced $\gamma\gamma$ invariant mass and the minimized log likelihood ratio $\ln(L_{\pi^0}/L_e)$.

The selected events are shown in fig. 5. A total of 28 ν_e candidate events are selected. The expected background is 4.92 ± 0.55 events. These results are based on 6.6×10^{20} POT.

Oscillation parameters are extracted from a maximum likelihood fit to the observed lepton $p-\theta$ distribution. Assuming the normal (inverted) hierachy, $\sin^2 2\theta_{13} = 0.140^{+0.038}_{-0.032}$ ($0.170^{+0.045}_{-0.037}$). The values of the other oscillation parameters are assumed to be $|\Delta m^2_{32}| = 2.4 \times 10^{-3} eV^2$, $\sin^2\theta_{23} = 0.5$, and $\delta_{CP} = 0$. The 68% and 90% CL for $\sin^2\theta_{13}$ evaluated for different values of δ_{CP} are shown in fig. 6. An alternative analysis based on the reconstucted neutrino energy distribution, assuming quasi-elastic kinematics, gives consistent results. The case of $\theta_{13} = 0$ is excluded at 7.3σ significance [10].

3.2 ν_μ Disappearance

A similar analysis is performed on the disappearance channel to measure $\sin^2(\theta_{23})$ and Δm^2_{32}. Fully contained, muon-like single ring events with visible energy > 30 MeV, reconstructed muon momentum > 200 MeV and ≤ 1 decay electron are selected.

The selected events are shown in fig. 7. 58 candidate ν_μ events are observed. With no oscillation 205 ± 17 events are expected. These results are based on 3.0×10^{20} POT.

A maximum likelihood fit to the reconstructed neutrino energy distribution assuming QE kinematics, gives $\sin^2(\theta_{23}) = 0.514 \pm 0.082$ and $\Delta m^2_{32} = 2.44^{+0.17}_{-0.15} \times 10^{-3} eV^2/c^4$. The 90% CL contour is shown in fig. 8 along with results from other experiments. This result is consistent with maximal disappearance probability [11].

4 Cross Section Measurements

Neutrino interactions on nuclei form the signal in all current and planned future long-baseline neutrino oscillation experiments. Understanding these interactions in the energy regime covered by the T2K beam flux is essential for the study of neutrino oscillations. The latest T2K cross section measurements in Charged Current (CC) Inclusive, CC quasi-elastic scattering (CCQE) and Neutral Currant Elastic (NCE) are shown in the following sections. These three measurements are based on the ND280 detector described in section 2.

4.1 CC Inclusive Cross Section Measurement

ν_μ CC interactions are selected by requiring events with a reconstructed μ^- starting within the FGD fiducial volume. Tracks are required to be negative, forward-going and have a muon-like TPC PID. This event selection achieves an efficiency of 50% and a purity of 87%. The dominant background is from out of fiducial volume interactions.

The cross section is extracted from the reconstructed $p_\mu - \cos(\theta_\mu)$ distribution. The NC background is subtracted and an efficiency correction is applied based on predictions from MC. An iterative Bayesian unfolding method is used to correct for reconstruction bias and unsmear distributions.

The measured double differential flux integrated cross section is shown in fig. 9 [12]. The flux-averaged total cross section is measured to be $\langle\sigma_{CC}\rangle_\phi = (6.91 \pm 0.13(stat) \pm 0.84(syst)) \times 10^{-39}\text{cm}^2/\text{nucleon}$ and is consistent with the predictions from NEUT [15] ($7.27 \times 10^{-39}\text{cm}^2/\text{nucleon}$) and GENIE [16] ($6.54 \times 10^{-39}\text{cm}^2/\text{nucleon}$) MC generators [12].

4.2 CCQE Cross Section

The Charged-Current Quasi-Elastic (CCQE) interaction, $\nu + n \rightarrow l^- + p$, is the main signal in the neutrino oscillation measurement. This two-body interaction is important because the initial neutrino energy can be inferred from final state lepton kinematics. Additional cuts are applied to the CC inclusive sample to select interactions containing a muon with no pions in the final state. This event selection achieves an efficiency of 40% and purity 72% for true CCQE events.

The CCQE cross section is extracted by fitting the NEUT MC model to the reconstructed $p_\mu - \cos(\theta_\mu)$ distribution. This is shown in Figure 10 [13]. Systematic uncertainties are accounted for by varying bin contents with nuisance parameters. A maximum likelihood fit is used to find the best fit parameters. A χ^2 test comparing the fitted result with the nominal NEUT model gives p-value of 17% indicating agreement between the data and the cross section model.

An alternative approach to fitting the cross-section normalisation, is to directly fit the model parameters. The axial mass parameter M_A^{QE} is varied to obtain the best fit to the observed data. The fit is performed once using both shape and normalisation and again using only shape information. The best fit values for M_A^{QE}-norm (M_A^{QE}-shape) with the RFG model is $1.14^{+0.27}_{-0.20}$ GeV ($1.38^{+0.39}_{-0.27}$ GeV). Large effective M_A^{QE} is believed to be due to unaccounted for nuclear effects. Note that the meaning of this effective parameter depends on the details of the QE model; comparison with results from other experiments should be done with care.

5 Neutral Current Elastic Cross Section Measurement

The Neutral Current Elastic channel is $\nu_\mu + p(n) \rightarrow \nu_\mu + p(n)$. The observable signal produced in the detector is a proton track. Note that cases where the target nucleon is a neutron can also produce protons due to final state interactions in the nucleus. In the T2K analysis the signal is defined as all NC interactions with only nucleons leaving the nucleus (no charged leptons or pions).

There are two main backgrounds to this channel. First, charged current interactions where the μ and p tracks are back-to-back and hence are reconstructed as the same track. This background is removed with PID based on dE/dx along the reconstructed track. Second, background from external interactions. This is measured in-situ from side-band samples.

3936 events are selected with an expect background of 2016. The flux integrated absolute cross section is calculated as $\langle\sigma\rangle_{\mathrm{flux}} = 2.24 \pm 0.07(\mathrm{stat})^{+0.53}_{-0.63}(syst) \times 10^{-39} cm^2$ [14]. This can be compared with MC predictions from NEUT (GENIE) of $\langle\sigma\rangle_{\mathrm{flux}} = 2.02(1.79) \times 10^{-39} cm^2$ This analysis is based on 9.9×10^{19}POT of water-in data. Future analyses will use water-out data to extract the cross-section on water.

6 Conclusion and Outlook

The T2K experiment has recorded 6.6×10^{20} POT recorded to date. With only a fraction of the approved POT, the T2K experiment has discovered ν_e appearance and is producing world leading measurements of the θ_{23} mixing angle. T2K will continue to improve the neutrino oscillation measurements and produce further neutrino interaction cross section measurements. In 2014 T2K will run for the first time in anti-neutrino mode. The observation of non-zero θ_{13} allows the measurement of δ_{CP}. The T2K experiment will lead the search for leptonic CP violation in the coming years.

References

[1] Z. Maki, M. Nakagawa, and S. Sakata, Prog. Theor. Phys. 28, 870 (1962).
[2] B. Pontecorvo, Sov. Phys. JETP 26, 984 (1968).
[3] K. Abe et al. (T2K Collaboration), Nucl. Instrum. Meth. A **659**, 106 (2011).
[4] N. Abgrall et al. (NA61/SHINE Collaboration), Phys.Rev. C84, 034604 (2011).
[5] N. Abgrall et al. (NA61/SHINE Collaboration), Phys.Rev. C85, 035210 (2012).
[6] K. Abe et al. (T2K Collaboration), Nucl. Instrum. Meth. A 694, 211 (2012).
[7] P.-A. Amaudruz et al. (T2K ND280 FGD Collaboration), Nucl. Instrum. Meth. A 696, 1 (2012).
[8] N. Abgrall et al. (T2K ND280 TPC Collaboration), Nucl. Instrum. Meth. A 637, 25 (2011).
[9] S. Assylbekov et al. (T2K ND280 P0D Collaboration), Nucl. Instrum. Meth. A 686, 48 (2012).
[10] K. Abe et al. (T2K Collaboration), arxiv:1311.4750 (2013)
[11] K. Abe et al. (T2K Collaboration), Phys. Rev. Lett. 111, 211803 (2013).
[12] K. Abe et al. (T2K Collaboration), Phys. Rev. D **87**, 092003 (2013).
[13] D. Hadley, Proceedings of NuFact 2013 (to appear)
[14] D. Ruterbories, Proceedings of NuFact 2013 (to appear)
[15] Y. Hayato, Acta Phys. Polon. B **40**, 2477 (2009).
[16] C.Andreopoulos et al., Nucl. Instrum. Meth. A **614** 87 (2010).

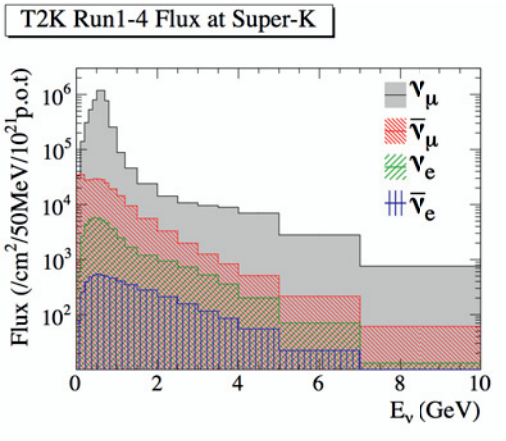

Figure 1: Predicted neutrino flux at SK.

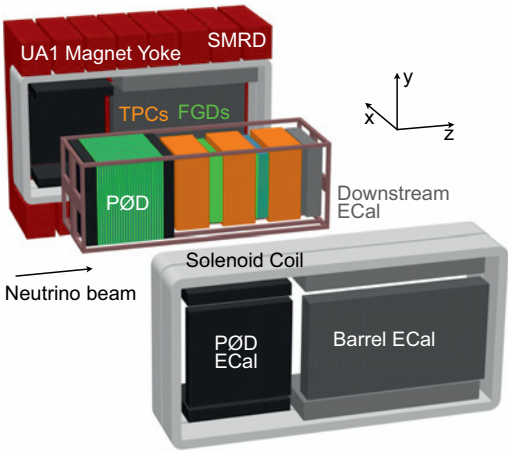

Figure 2: The ND280 off axis near detector.

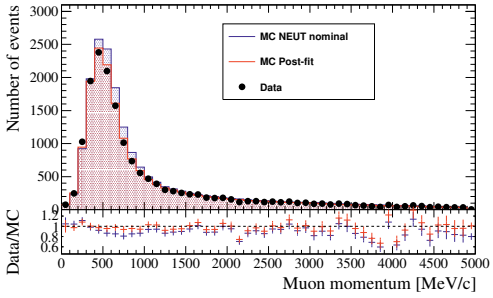

(a) $CC0\pi$

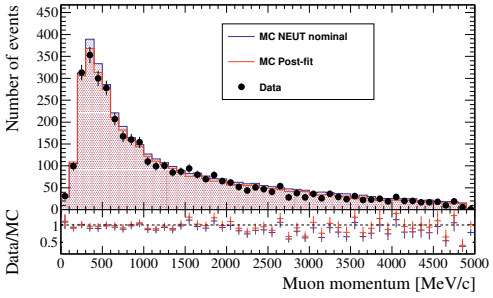

(b) $CC1\pi$

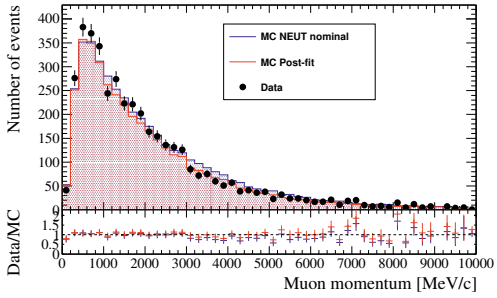

(c) CC other

Figure 3: The reconstructed muon momentum distribution for the 3 ND280 samples (a) $CC0\pi$ (b) $CC1\pi$ and (c) CC other. The MC predictions are shown both before and after fitting.

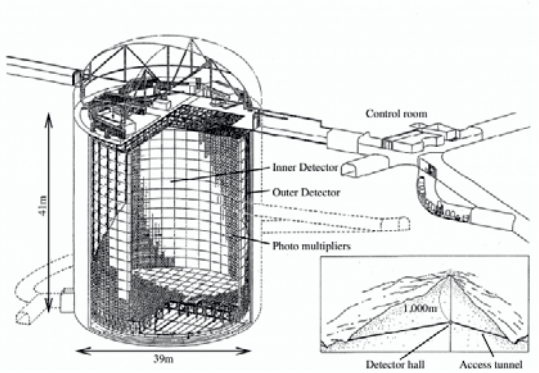

Figure 4: The Super-K detector.

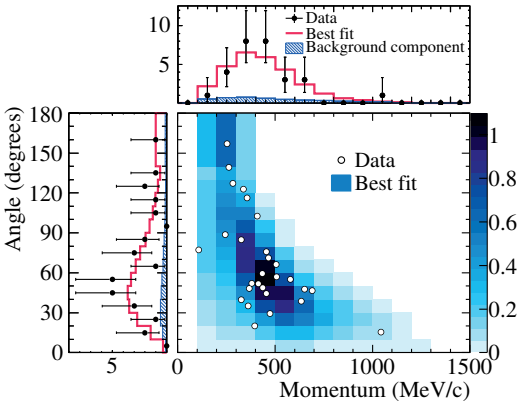

Figure 5: The reconstructed $p - \theta$ distribution of the ν_e candidate events in SK. The 1D projection of each variable is also shown along each axis.

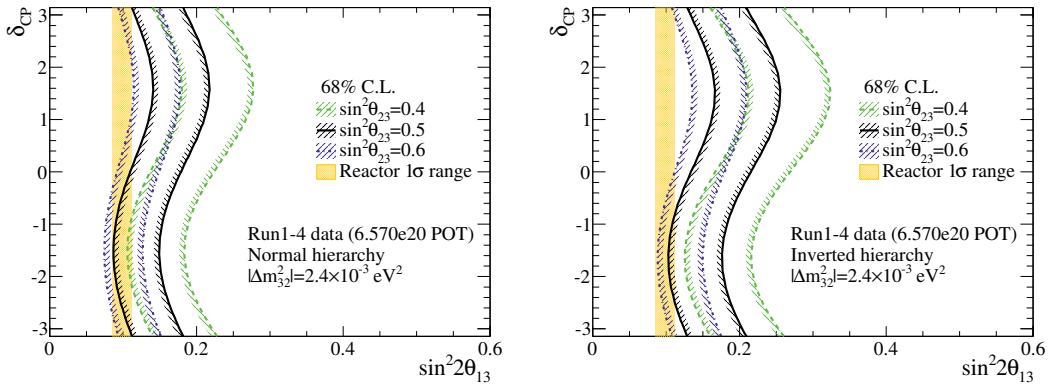

Figure 6: The 68% CL contours on $\sin^2 2\theta_{13}$ evaluated for different values of δ_{CP} and with different assumptions of the value of θ_{23}. The constraint from reactor experiments is overlaid.

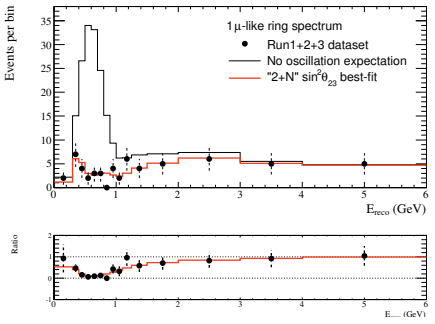

Figure 7: The reconstructed neutrino energy of the candidate ν_μ events in SK.

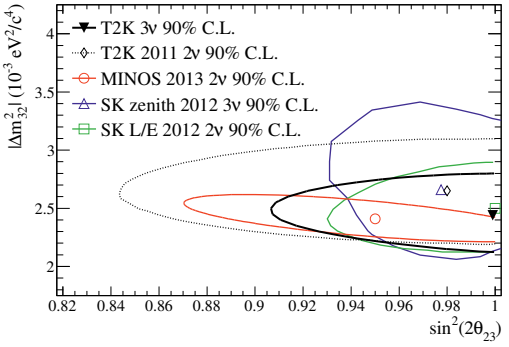

Figure 8: 90% CL on $\sin^2 2\theta_{23}$ and $|\Delta m^2_{32}|$ Results from other experiments are shown for comparison. .

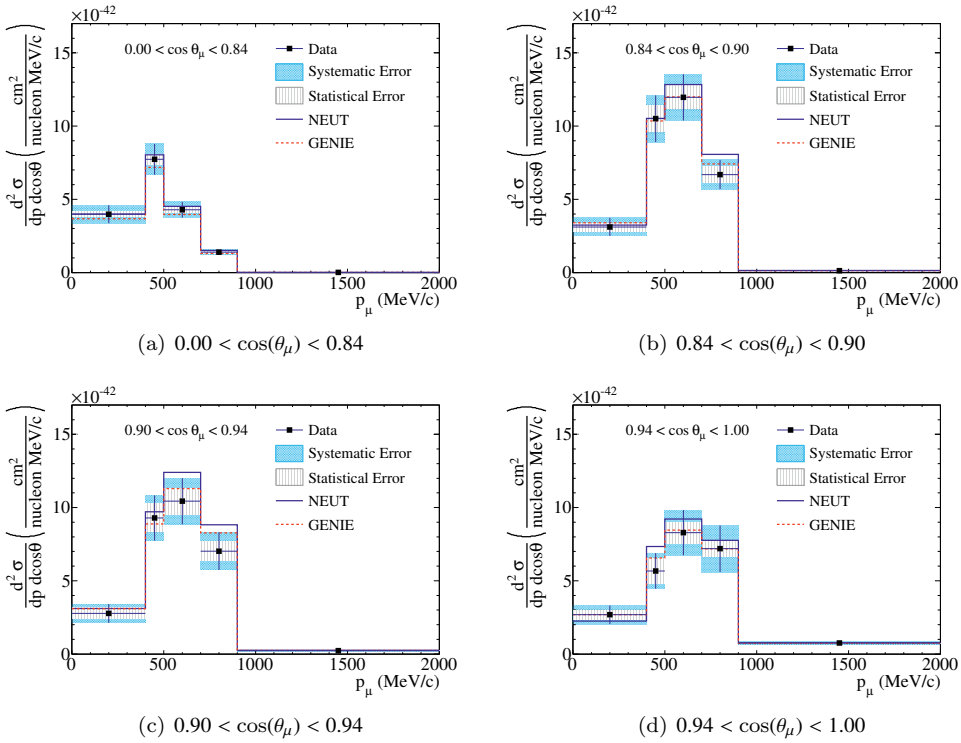

(a) $0.00 < \cos(\theta_\mu) < 0.84$ (b) $0.84 < \cos(\theta_\mu) < 0.90$

(c) $0.90 < \cos(\theta_\mu) < 0.94$ (d) $0.94 < \cos(\theta_\mu) < 1.00$

Figure 9: The measured CC inclusive cross section. Figures (a-d) show the μ^- momentum distribution in each bin of $\cos(\theta_\mu)$. The ND280 result is shown along side the prediction from the NEUT and GENIE neutrino event generators.

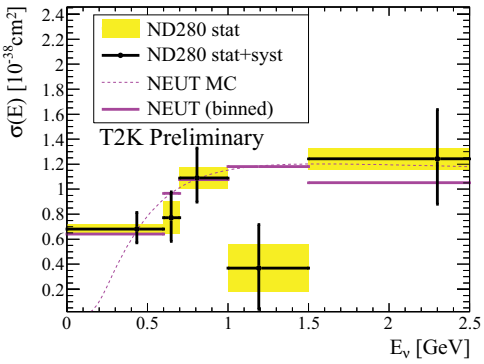

Figure 10: The measured CCQE cross section.